COO-2490-8

DIFFERENTIAL SCATTERING CROSS SECTIONS OF LITHIUM 6 AND LITHIUM 7 FOR NEUTRONS OF 4 TO 7.5 MeV ENERGY

H.D. Knox, R.M. White, and R.O. Lane

June 1978

Study of Structure of Light Nuclei with Neutrons

Ohio University

Athens, Ohio

DISCLAIMER

COO-2490-8

DIFFERENTIAL SCATTERING CROSS SECTIONS OF LITHIUM 6 AND LITHIUM 7 FOR NEUTRONS OF 4 TO 7.5 MEV ENERGY

H.D. Knox, R.M. White and R.O. Lane

Ohio University, John E. Edwards Accelerator Laboratory
Athens, Ohio

MASTER

June 1978

PREPARED FOR THE U.S. DEPARTMENT OF ENERGY

UNDER CONTRACT EY-76-02-2490

NOTICE

This report was prepared as an account of work sponsored by the United States Government. Neither the United States nor the United States Department of Energy, nor any of their employees, nor any of their contractors, sub-contractors, or their employees, makes any warranty, express or implied, or assumes any legal liability or responsibility for the accuracy, completeness, or usefulness of any information, apparatus, product or process disclosed or represents that its use would not infringe privately owned rights.

Differential Scattering Cross Sections of Lithium 6 and Lithium 7 for Neutrons of 4 to 7.5 MeV Energy*

H.D. Knox, R.M. White and R.O. Lane

Ohio University, John E. Edwards Accelerator Laboratory
Athens, Ohio 45701

ABSTRACT

Differential cross sections for neutrons scattered elastically from ^{6}Li and ^{7}Li have been measured at 14 incident neutron energies between 4 and 7.5 MeV. For ^{7}Li, neutrons inelastically scattered from the 0.478 MeV level were not resolved from the elastic group and have been included with the elastic group in calculating the cross sections. The present ^{6}Li data are in good agreement with the ENDF/B-IV evaluation while the present $^{7}Li(n,n_0+n_1)$ data are generally larger than the corresponding ENDF/B-IV evaluation particularly at forward angles.

*Work supported by U.S. Department of Energy.

INTRODUCTION

Accurate knowledge of neutron cross sections of both ^{6}Li and ^{7}Li is needed up to 14 MeV incident energy since both of these isotopes are to be used in breeding blankets of proposed fusion reactors. Also a detailed data base is needed for evaluation work on ^{6}Li because of its use as a primary neutron standard. Two measurements of neutron differential elastic cross sections have been reported in the 4 to 7.5 MeV region--these are by Hopkins, Drake and Conde[1)] and by Batchelor and Towle.[2)] In both of these works only a few distributions were reported and comparisons between the two data sets are difficult since measurements were not made at overlapping energies. Measurements of the differential cross section of neutrons scattered from both ^{6}Li and ^{7}Li in this energy range have been completed at the Ohio University Tandem Accelerator Laboratory. These measurements were undertaken first, to provide a more complete and detailed data base in this energy region, and second, to provide checks of the previously reported data. Measurements were, therefore, taken at 14 incident energies including those energies overlapping with all measurements of both Hopkins et al.[1)] and Batchelor and Towle.[2)]

EXPERIMENTAL PROCEDURE AND DATA ANALYSIS

These measurements were made with the neutron time-of-flight facility at the Ohio University Tandem Accelerator Laboratory. Descriptions of this facility and methods of data acquisition and analysis have been reported previously[3,4] and only a brief description will be given here.

Neutrons were produced by a pulsed proton beam striking a tritium gas cell. Proton energy loss in the cell was the primary source of energy spread in the neutron burst and amounted to 40 to 80 keV.

The scattering samples were composed of lithium metal enclosed in thin-walled aluminum cans. The ^{6}Li sample was 15.06 gms of 99% lithium by weight with an isotopic composition of 95.1% ^{6}Li. The ^{7}Li sample was 17.03 gms of 99% natural lithium by weight with an isotopic composition of 92.5% ^{7}Li. Both samples were 3.396 cm in diameter. The ^{6}Li sample was 3.705 cm high while the ^{7}Li sample was 3.595 cm high. An empty can identical to those containing the lithium samples was used for sample-out runs.

The main neutron detector was a 5-cm thick x 18-cm-diameter NE-224 liquid scintillator, optically coupled to an RCA 4522 photomultiplier tube. This detector was located 3.6 m from the scattering sample inside a massive neutron collimated shield. A monitor detector consisting of a thin NE 102 plastic scintillator coupled to an RCA 8575 photomultiplier tube was located at 25° with respect to the incident proton beam. Relative efficiencies of the two detectors were determined by placing the main detector at zero degrees and with the monitor at its fixed position, recording charge-normalized counts in each detector at neutron energies to be encountered during the actual experiment. In normal data taking, detector counts were then normalized to the monitor. The conversion of counts to absolute cross section was accomplished by using ratios of the well-known zero-degree yield of the T(p,n)^{3}He reaction at one energy compared to another.

Differential cross sections for ^{6}Li and ^{7}Li were measured at nine laboratory angles between 20 and 160 degrees for 14 incident neutron energies between 4 and 7.5 MeV. Interspersed with these lithium measurements were determinations of the differential cross sections of neutrons scattered from ^{12}C at 4.08, 5.05 and 6.94 MeV. These carbon measurements are made routinely during any series of differential cross section measurements in this energy region. Comparisons with earlier measurements at this laboratory[3)] and other laboratories[5)] provide checks of the entire system throughout this energy range.

Neutrons inelastically scattered from the 0.478 MeV level in ^{7}Li were not completely resolved from the elastic group. This incomplete separation was caused in part by the ^{6}Li contaminant(7.5%) in the ^{7}Li scattering sample. Neutrons elastically scattered from the ^{6}Li minor isotope kinematically fall between the ^{7}Li elastic and inelastic groups making complete separation impossible. In the present results neutrons inelastically scattered from the 0.478 MeV level have been included with the elastic group in computing the differential cross section. The differences in detector efficiencies for the elastic and inelastic groups have been accounted for in the calculation of the resulting composite cross sections. Further inelastic measurements are planned at this laboratory using new highly enriched ^{6}Li and ^{7}Li scattering samples.

The present data have been corrected for the effects of finite geometry, attenuation, air scattering, minor isotope contamination and multiple scattering. The largest of these, multiple scattering and finite geometry were typically 5 to 10%.

RESULTS AND DISCUSSION

The present results for ^{6}Li and ^{7}Li are shown in Figures 1 and 2 in the form of Legendre polynomial expansion coefficients for the differential scattering cross section. In both figures energies are given in the laboratory system. The coefficients for ^{6}Li are slowly varying with energy indicating very little resonance structure. Two broad resonances are seen in the ^{7}Li(n,n_0+n_1) channel, probably caused by levels at excitation energies of E_x = 6.1 and 7.1 MeV in the ^{8}Li system.

Comparisons of the present results with those of Hopkins et al.[1)] are shown in Figure 3 for ^{6}Li and Figure 4 for ^{7}Li. In these figures and all figures to follow, error bars are not shown if they are smaller than the symbols. For comparison with the present ^{7}Li + n measurements the differential elastic and inelastic cross sections of Hopkins *et al*.[1)] have been summed. In both figures the solid curves are least squares Legendre polynomial fits to the present data. The agreement between the two experiments is excellent at all energies.

Comparisons of the present results with those of Batchelor and Towle[2)] are shown in Figure 5 for ^{6}Li and in Figure 6 for ^{7}Li. Fully corrected values of the actual experimental data points of Reference 2 are not available. Instead, they present tabulated differential cross sections at an arbitrary set of angles which were based on a fitted curve which, in turn, had been corrected for multiple scattering and finite geometry. In Figure 5 the solid curve is a least squares fit of the tabulated data of Reference 2 for ^{6}Li. The agreement between this curve and the present experimental data is generally good. For ^{7}Li, Batchelor and Towle[2)] obtained values for the elastic cross section by subtracting estimates of the differential inelastic cross sections from their corrected distributions. For purposes of comparison with the present ^{7}Li results, these estimates were added back again to the tabulated elastic results of Reference 2 to give the $^7Li(n,n_0+n_1)$ differential cross sections. The solid curves in Figure 6 are least squares fits to the results for $^7Li(n,n_1+n_0)$ derived from Reference 2 in this manner. Except at 7.5 MeV, the present data tend to be higher than the results of Batchelor and Towle[2) particularly at forward angles.

Comparisons of the present ^{6}Li differential cross sections with the current ENDF/B-IV evaluations are shown in Figure 7 and the integrated ^{6}Li cross sections are shown in Figure 8. The agreement for both differential and integrated cross sections with ENDF/B-IV is excellent. Similar comparisons for ^{7}Li are shown in Figures 9 and 10 respectively. Except at the highest energy the evaluated differential cross sections tend to be lower than the present data particularly at the forward angles and this is reflected in the integrated values.

Differential cross sections for 1.5 to 4 MeV neutrons scattered from ^{6}Li have been recently measured by A.B. Smith[6) at Argonne National Laboratory. Two measurements were made by Smith[6) at 4.00 MeV. These results are shown in Figure 11 along with the present data at 4.08 MeV. The solid curve is a least squares Legendre polynomial fit to the present data. The two measurements by Smith,[6) labeled "Data Set 1" and "Data Set 2" in Figure 11, were made using scattering samples of different size. The errors associated with Data Set 1, made with a very small scattering sample, are approximately twice those of Data Set 2. At forward angles, the present data and those of Smith[6) agree very well, while those of Smith[6) are slightly higher at backward angles.

Differential cross sections for neutrons scattered from both ^{6}Li and ^{7}Li have been measured at Duke University by F.O. Purser[7) for $7.0 \leq E_n \leq 15$ MeV. A comparison of the present results with the Duke results is shown in Figure 12. The agreement is excellent.

The results from Argonne,[6] Duke University,[7] the present work, and the earlier work by Lane et al.[8] provide differential cross sections for the lithium isotopes up to 15 MeV. In each of these experiments sufficient energy overlap was allowed for comparisons with the data of other experiments. With the excellent comparisons seen here, the combined results provide consistent and detailed measurements throughout the range of energies where data is needed for fusion energy applications.

ACKNOWLEDGEMENTS

The authors wish to express their sincere appreciation to Donald Carter and David Sturbois of the Laboratory Staff whose extra efforts and assistance in this work were essential to its successful completion.

REFERENCES

1. J.C. Hopkins, D.M. Drake and H. Conde, Nucl. Phys. A107, 139 (1968).

2. R. Batchelor and J. Towle, Nucl. Phys. 47, 385 (1963).

3. R.M. White, "A Study of the Higher Excitation States of ^{12}B via the $^{11}B(n,n)^{11}B$ Reaction," COO-2490-6, Ohio University Tandem Accelerator Laboratory (1977).

4. H.D. Knox, R.M. White, and R.O. Lane, Nucl. Sci. Eng. 65, 65 (1978).

5. W. Galati, J.D. Brandenberger and J.L. Weil, Phys. Rev. C5, 1508 (1972).

6. A.B. Smith, private communication.

7. E.B. Bilpuch, D.H. Epperson, D.W. Glasgow, S.G. Glendinning, C.R. Gould, H.H. Hogue, P.W. Lisowski, C.E. Nelson, H.W. Newson, F.O. Purser, L.W. Seagondollar, W. Tornow, and P. von Behren, Proc. of the Intl. Conf. on the Interactions of Neutrons with Nuclei, E.R.D.A. CONF-760715-P2, p. 1309.

8. R.O. Lane, A.J. Elwyn, and A. Langsdorf, Jr., Phys. Rev. 136, B1710 (1964).

FIGURE CAPTIONS

Figure 1. Legendre polynomial expansion coefficients of the present ^{6}Li + n data versus neutron energy. The coefficients represent center-of-mass cross sections while neutron energies are in the laboratory system.

Figure 2. Legendre polynomial expansion coefficients of the present ^{7}Li(n,n_0+n_1) data versus incident neutron energy. The coefficients represent center-of-mass cross sections while neutron energies are in the laboratory system.

Figure 3. Comparisons of the present ^{6}Li + n data with the measurements of Hopkins *et al*. (Reference 1). The solid curve is a least squares Legendre polynomial fit to the present data.

Figure 4. Comparisons of the present ^{7}Li(n,n_0+n_1) data with the measurements of Hopkins *et al*. (Reference 1). The solid curve is a least squares Legendre polynomial fit to the present data.

Figure 5. Comparisons of the present ^{6}Li + n data with the evaluated results of Batchelor and Towle (Reference 2). The solid curves are least squares Legendre polynomial fits to the numerical cross sections obtained by Batchelor and Towle.

Figure 6. Comparisons of the present ^{7}Li(n,n_0+n_1) data with the evaluated results of Batchelor and Towle (Reference 2). The solid curves are least squares Legendre polynomial fits to the numerical cross sections obtained by adding the inelastic cross sections of Batchelor and Towle to their tabulated elastic cross sections.

Figure 7. Comparisons of the present ^{6}Li + n differential data with the ENDF/B-IV evaluation.

Figure 8. Comparison of the integrated elastic cross sections for ^{6}Li + n of the present work, Hopkins _et al_. (Reference 1), Batchelor and Towle (Reference 2) and the ENDF/B-IV evaluation.

Figure 9. Comparisons of the present ^{7}Li(n,n_0+n_1) differential data with the ENDF/B-IV evaluation.

Figure 10. Comparison of the integrated ^{7}Li(n,n_0+n_1) cross sections of the present work, Hopkins _et al_. (Reference 1), Batchelor and Towle (Reference 2) and the ENDF/B-IV evaluation.

Figure 11. Comparison of the present ^{6}Li + n experimental results with those of A. Smith (Reference 6). The solid curve is a least squares polynomial fit to the present data.

Figure 12. Comparison of the present results with the Duke results (Reference 7). The solid curve is a least squares Legendre polynomial fit to the present data.

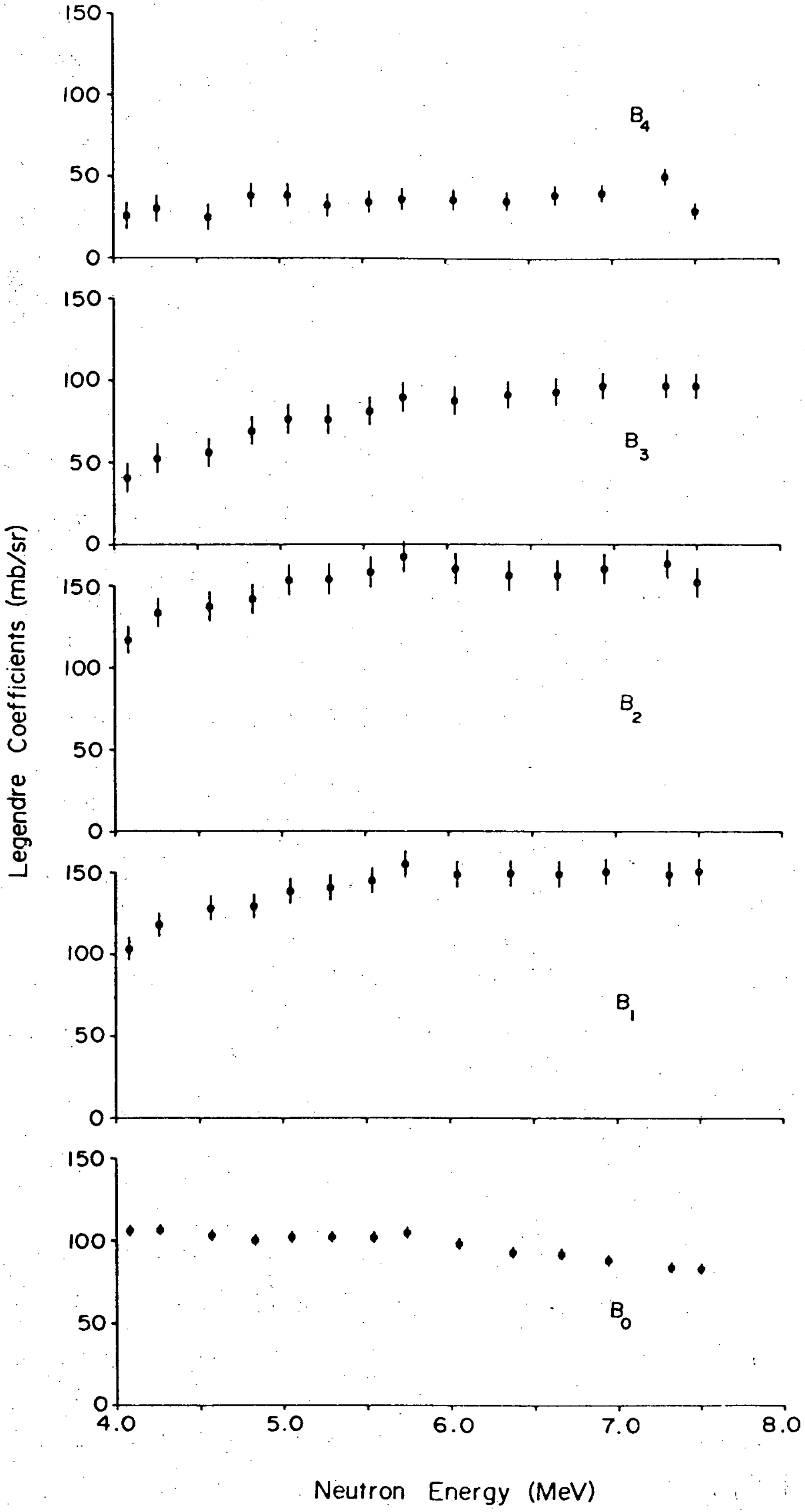
B4
B3
B2
B1
B0
Legendre Coefficients (mb/sr)
Neutron Energy (MeV)

Figure 1.

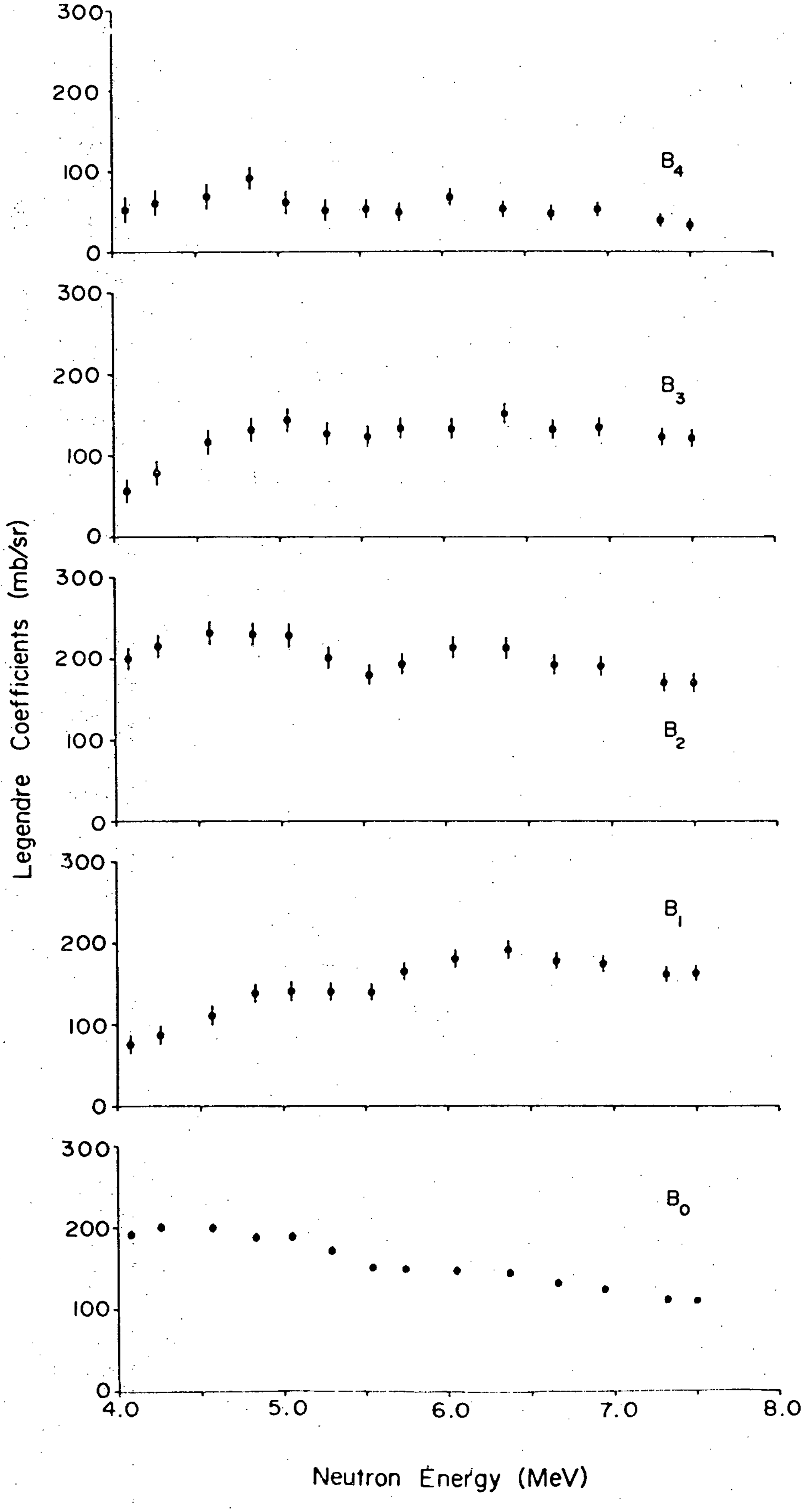
Legendre Coefficients (mb/sr)
Neutron Energy (MeV)
B_4
B_3
B_2
B_1
B_0
0
100
200
300
4.0
5.0
6.0
7.0
8.0

Figure 2.

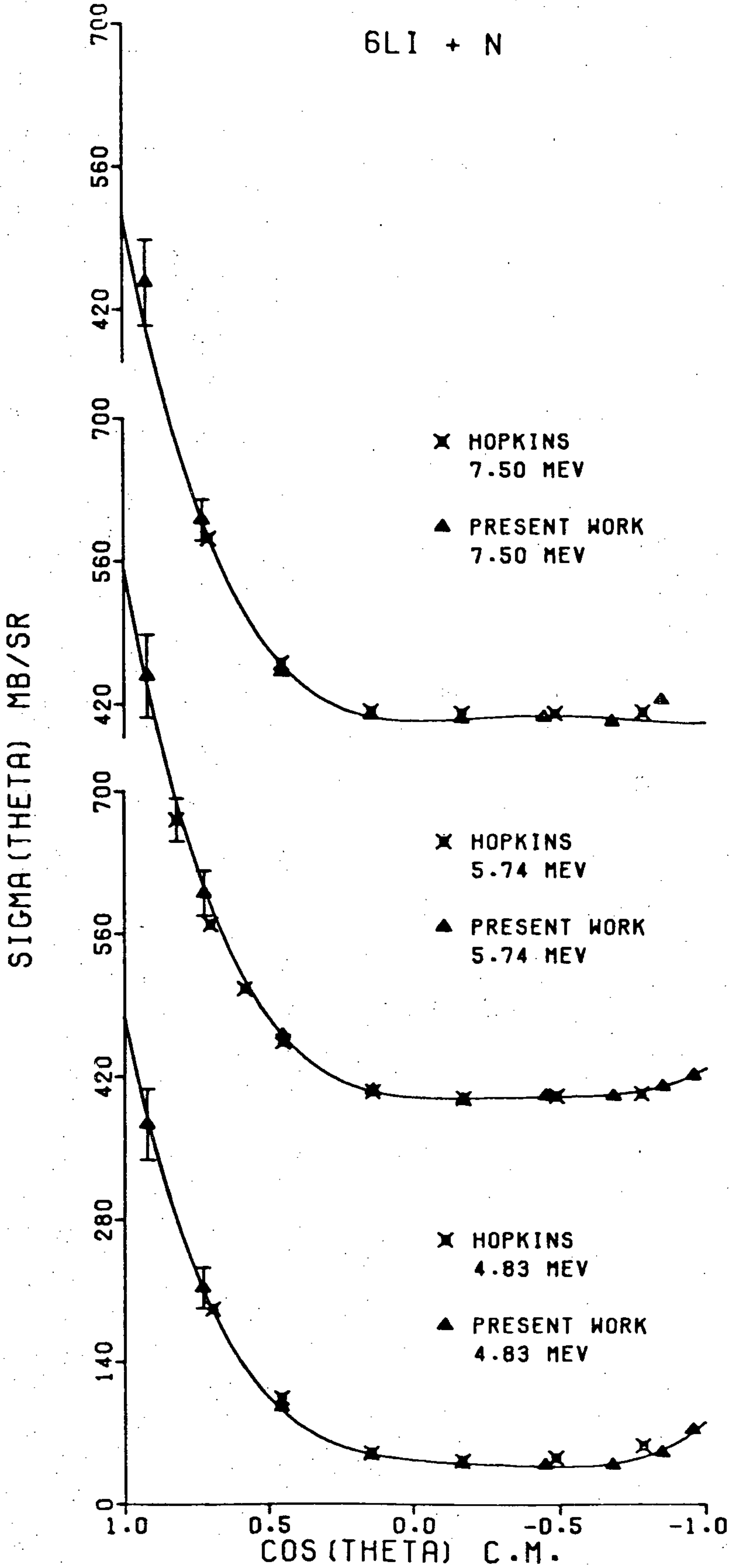
6LI + N
HOPKINS 7.50 MEV
PRESENT WORK 7.50 MEV
HOPKINS 5.74 MEV
PRESENT WORK 5.74 MEV
HOPKINS 4.83 MEV
PRESENT WORK 4.83 MEV
SIGMA(THETA) MB/SR
COS(THETA) C.M.
700
560
420
280
140
0
1.0
0.5
0.0
-0.5
-1.0

Figure 3.

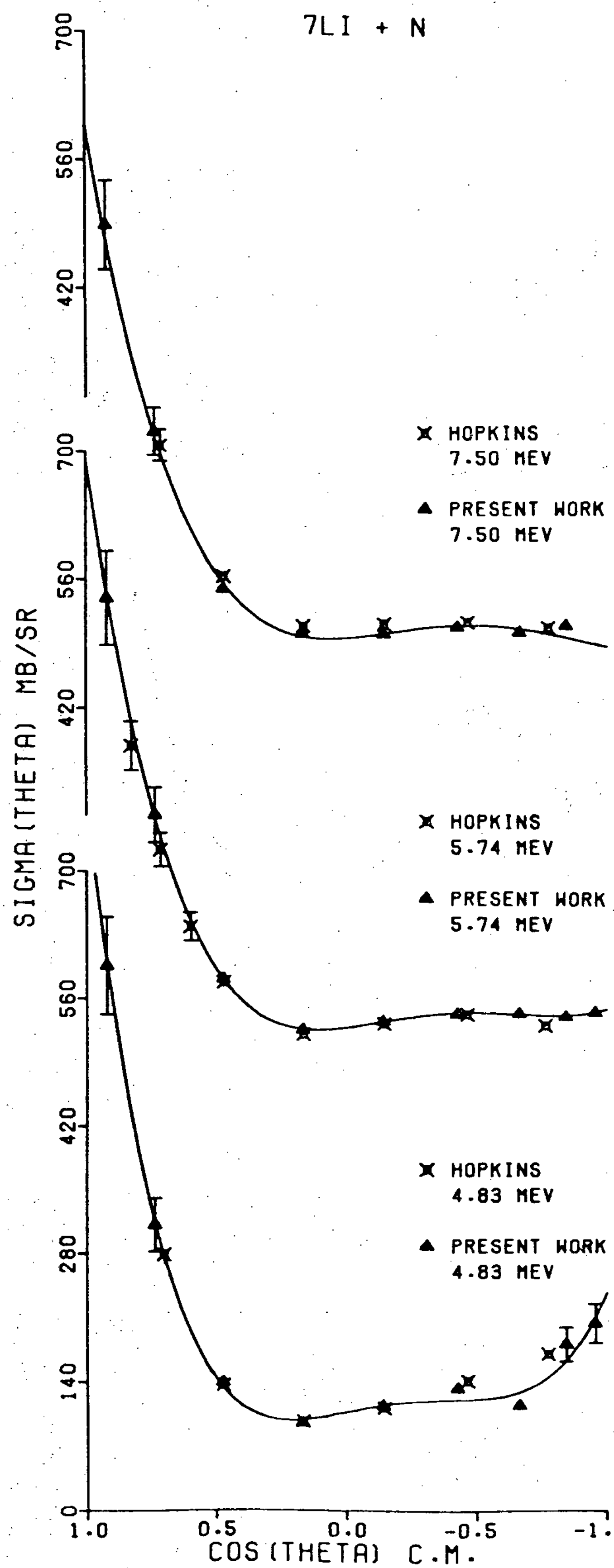
7LI + N
SIGMA(THETA) MB/SR
COS(THETA) C.M.
HOPKINS 7.50 MEV
PRESENT WORK 7.50 MEV
HOPKINS 5.74 MEV
PRESENT WORK 5.74 MEV
HOPKINS 4.83 MEV
PRESENT WORK 4.83 MEV
700
560
420
280
140
0
1.0
0.5
0.0
-0.5
-1.0

Figure 4.

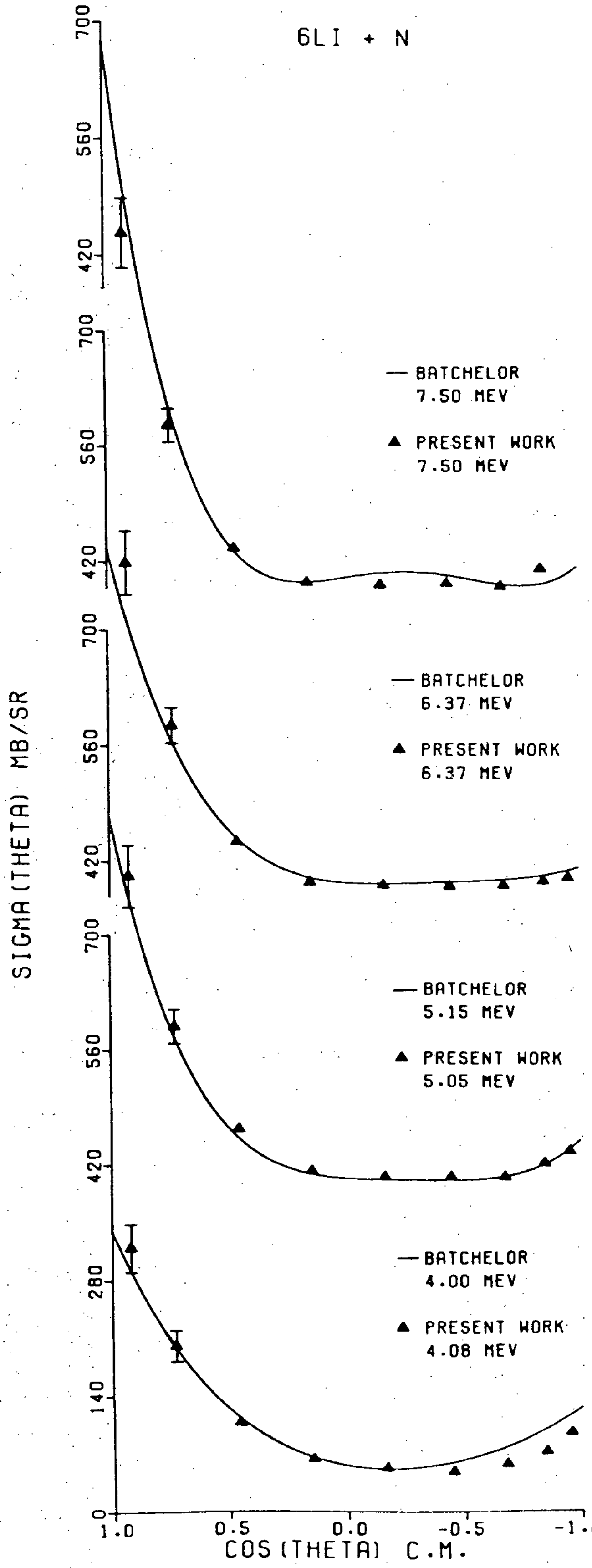

6LI + N
SIGMA(THETA) MB/SR
COS(THETA) C.M.
BATCHELOR
7.50 MEV
PRESENT WORK
7.50 MEV
BATCHELOR
6.37 MEV
PRESENT WORK
6.37 MEV
BATCHELOR
5.15 MEV
PRESENT WORK
5.05 MEV
BATCHELOR
4.00 MEV
PRESENT WORK
4.08 MEV
700
560
420
280
140
0
1.0
0.5
0.0
-0.5
-1.0

Figure 5.

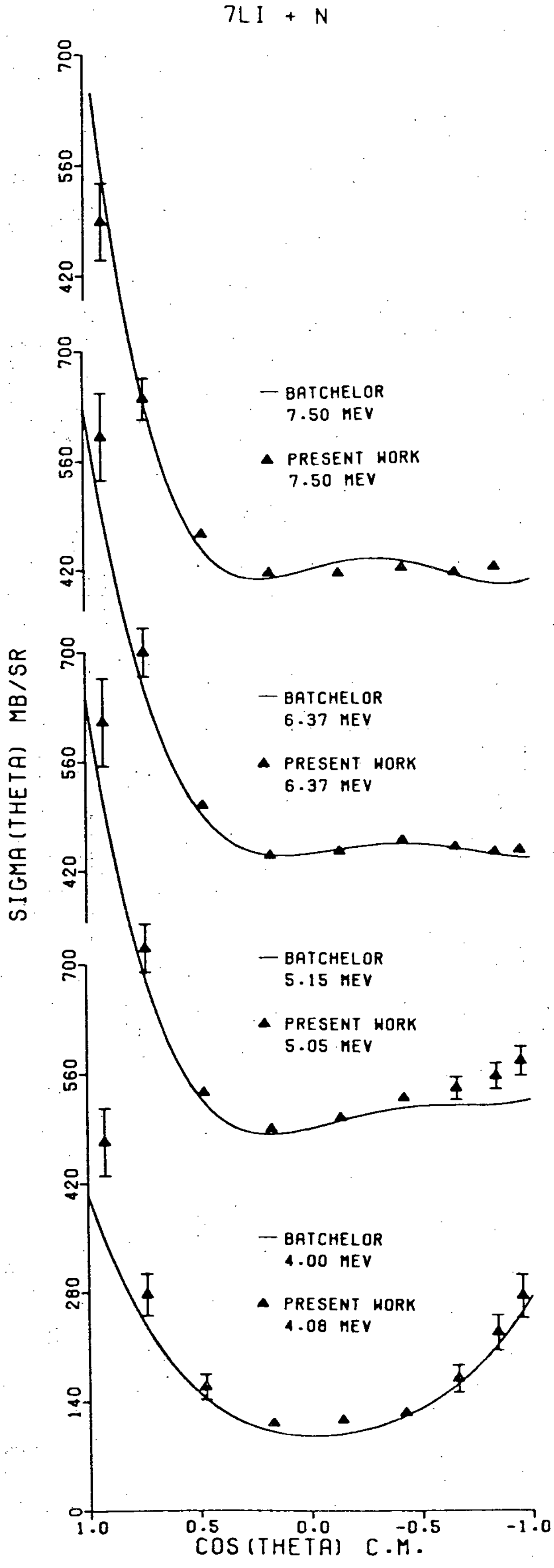

7LI + N
SIGMA(THETA) MB/SR
COS(THETA) C.M.
700
560
420
280
140
0
1.0
0.5
0.0
-0.5
-1.0
— BATCHELOR
7.50 MEV
▲ PRESENT WORK
7.50 MEV
— BATCHELOR
6.37 MEV
▲ PRESENT WORK
6.37 MEV
— BATCHELOR
5.15 MEV
▲ PRESENT WORK
5.05 MEV
— BATCHELOR
4.00 MEV
▲ PRESENT WORK
4.08 MEV

Figure 6.

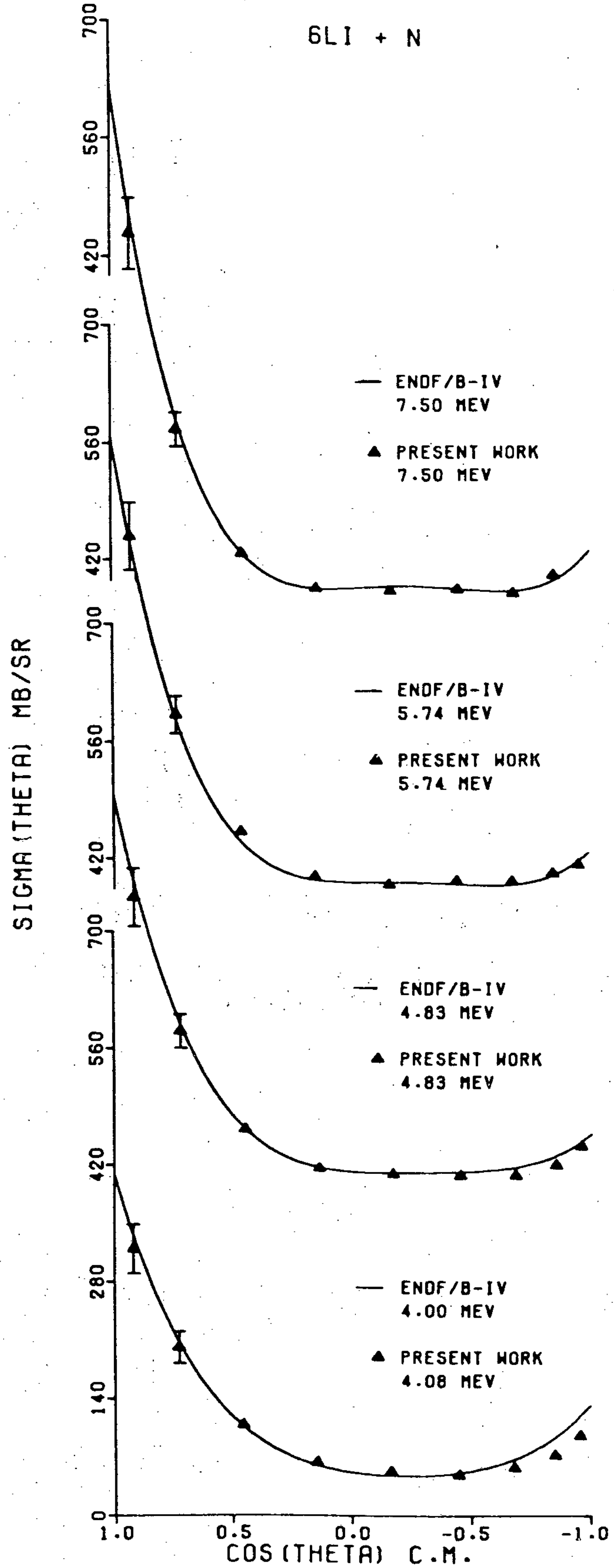
6LI + N
ENDF/B-IV
7.50 MEV
PRESENT WORK
7.50 MEV
ENDF/B-IV
5.74 MEV
PRESENT WORK
5.74 MEV
ENDF/B-IV
4.83 MEV
PRESENT WORK
4.83 MEV
ENDF/B-IV
4.00 MEV
PRESENT WORK
4.08 MEV
SIGMA(THETA) MB/SR
COS(THETA) C.M.
700
560
420
280
140
0
1.0
0.5
0.0
-0.5
-1.0

Figure 7.

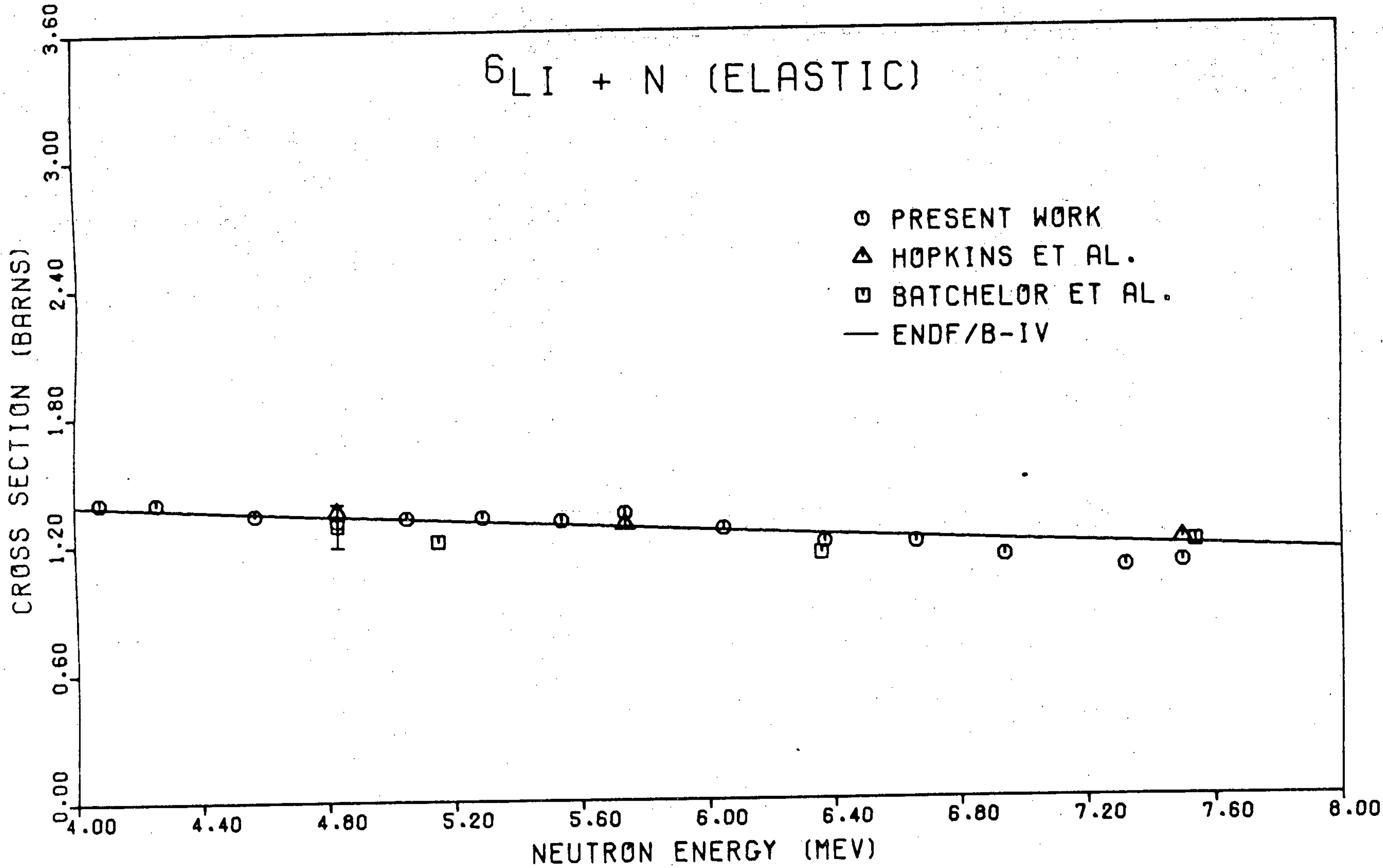
6LI + N (ELASTIC)
PRESENT WORK
HOPKINS ET AL.
BATCHELOR ET AL.
ENDF/B-IV
CROSS SECTION (BARNS)
0.00
0.60
1.20
1.80
2.40
3.00
3.60
4.00
4.40
4.80
5.20
5.60
6.00
6.40
6.80
7.20
7.60
8.00
NEUTRON ENERGY (MEV)

Figure 8.

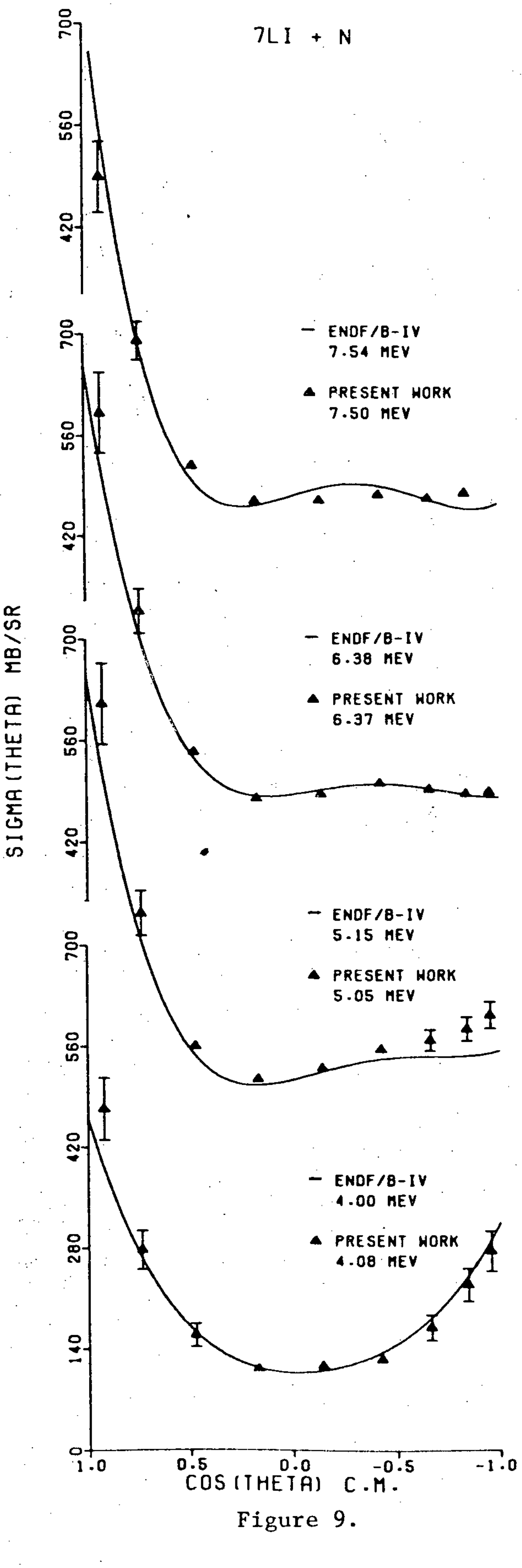
7LI + N
SIGMA(THETA) MB/SR
700
560
420
280
140
0
ENDF/B-IV
7.54 MEV
PRESENT WORK
7.50 MEV
ENDF/B-IV
6.38 MEV
PRESENT WORK
6.37 MEV
ENDF/B-IV
5.15 MEV
PRESENT WORK
5.05 MEV
ENDF/B-IV
4.00 MEV
PRESENT WORK
4.08 MEV
1.0
0.5
0.0
-0.5
-1.0
COS(THETA) C.M.

Figure 9.

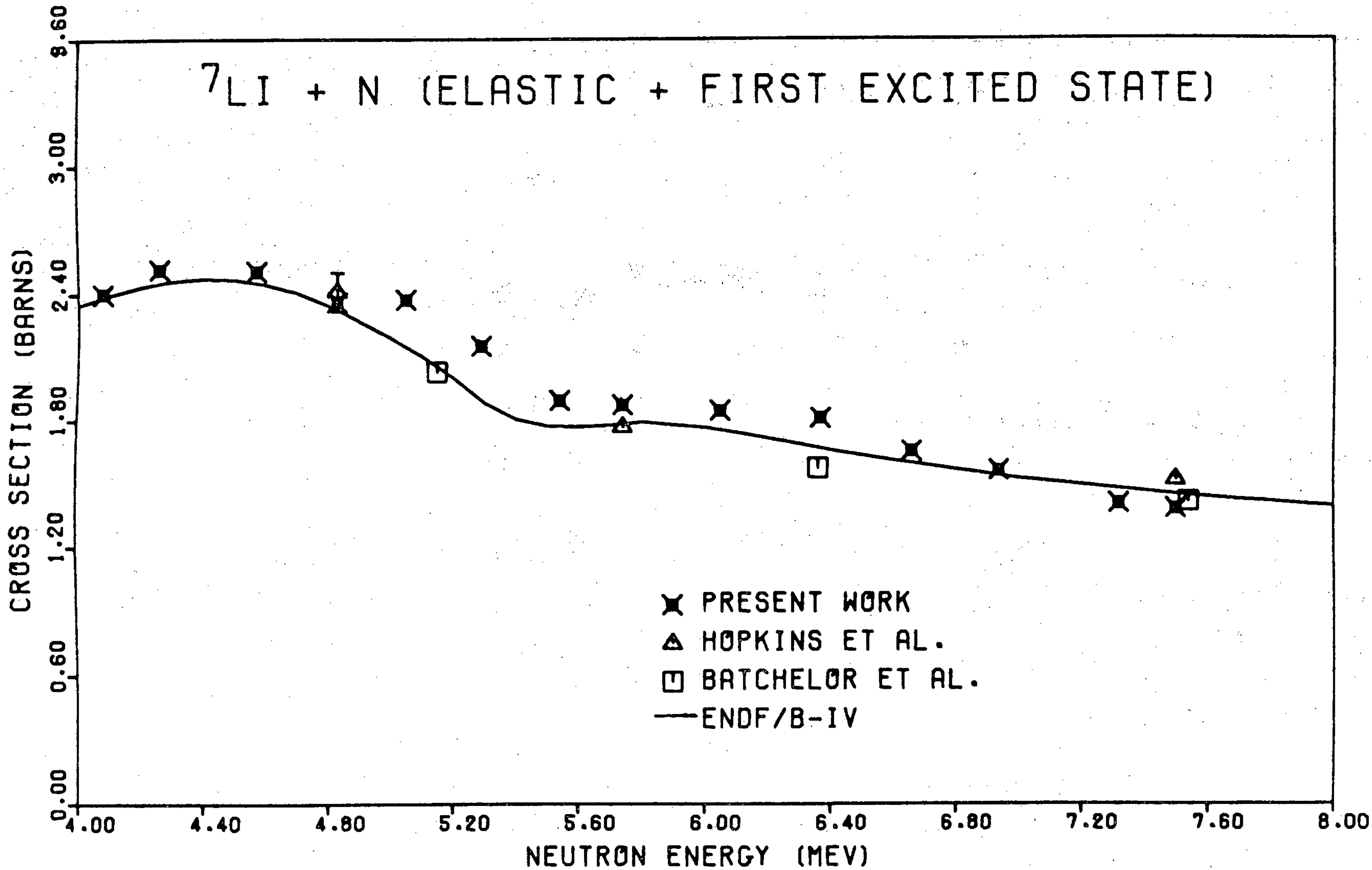

7LI + N (ELASTIC + FIRST EXCITED STATE)
CROSS SECTION (BARNS)
0.00
0.60
1.20
1.80
2.40
3.00
3.60
4.00
4.40
4.80
5.20
5.60
6.00
6.40
6.80
7.20
7.60
8.00
NEUTRON ENERGY (MEV)
PRESENT WORK
HOPKINS ET AL.
BATCHELOR ET AL.
ENDF/B-IV

Figure 10.

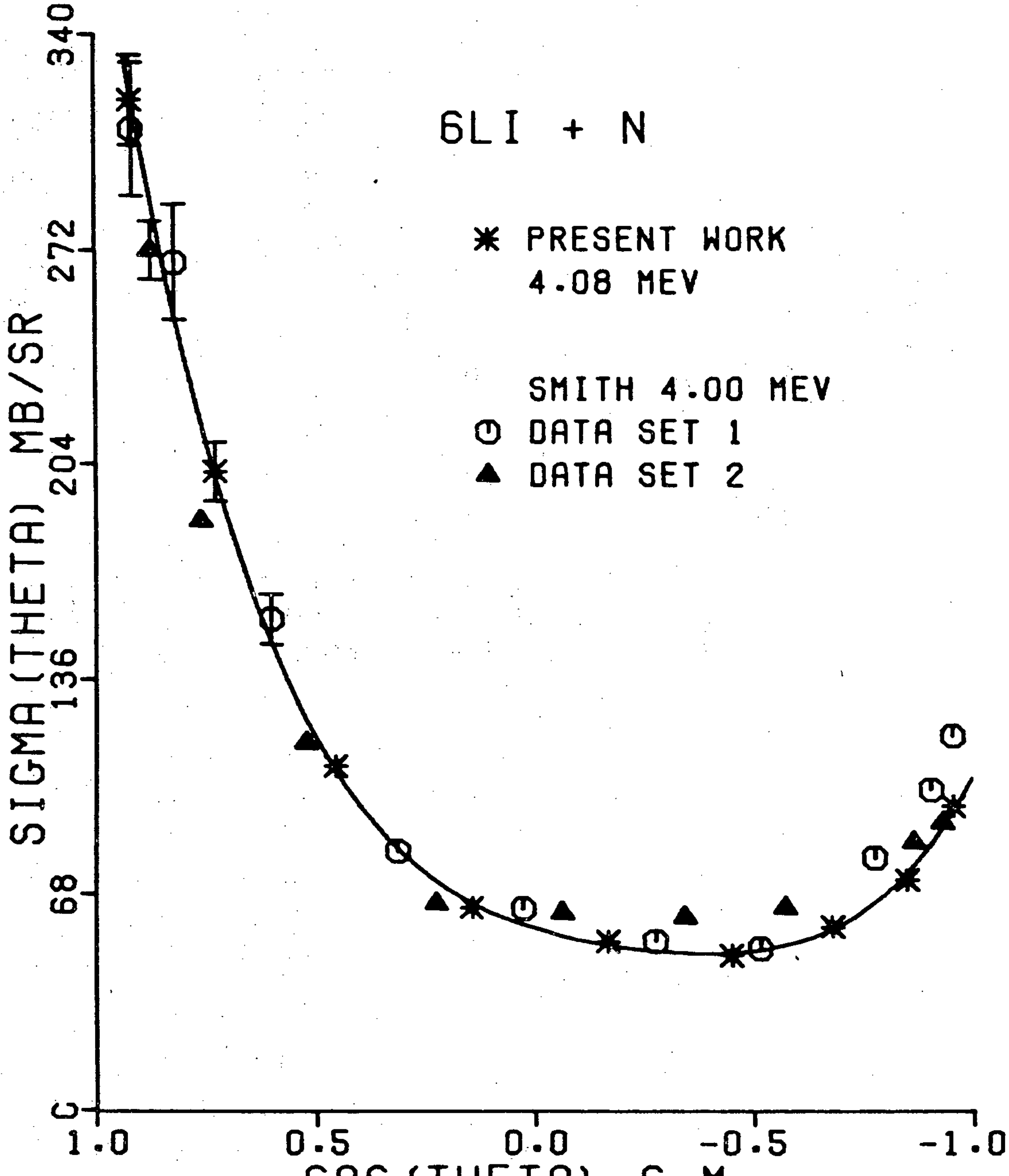

6LI + N
PRESENT WORK
4.08 MEV
SMITH 4.00 MEV
DATA SET 1
DATA SET 2
340
272
204
136
68
0
SIGMA(THETA) MB/SR
1.0
0.5
0.0
-0.5
-1.0
COS(THETA) C.M.

Figure 11.

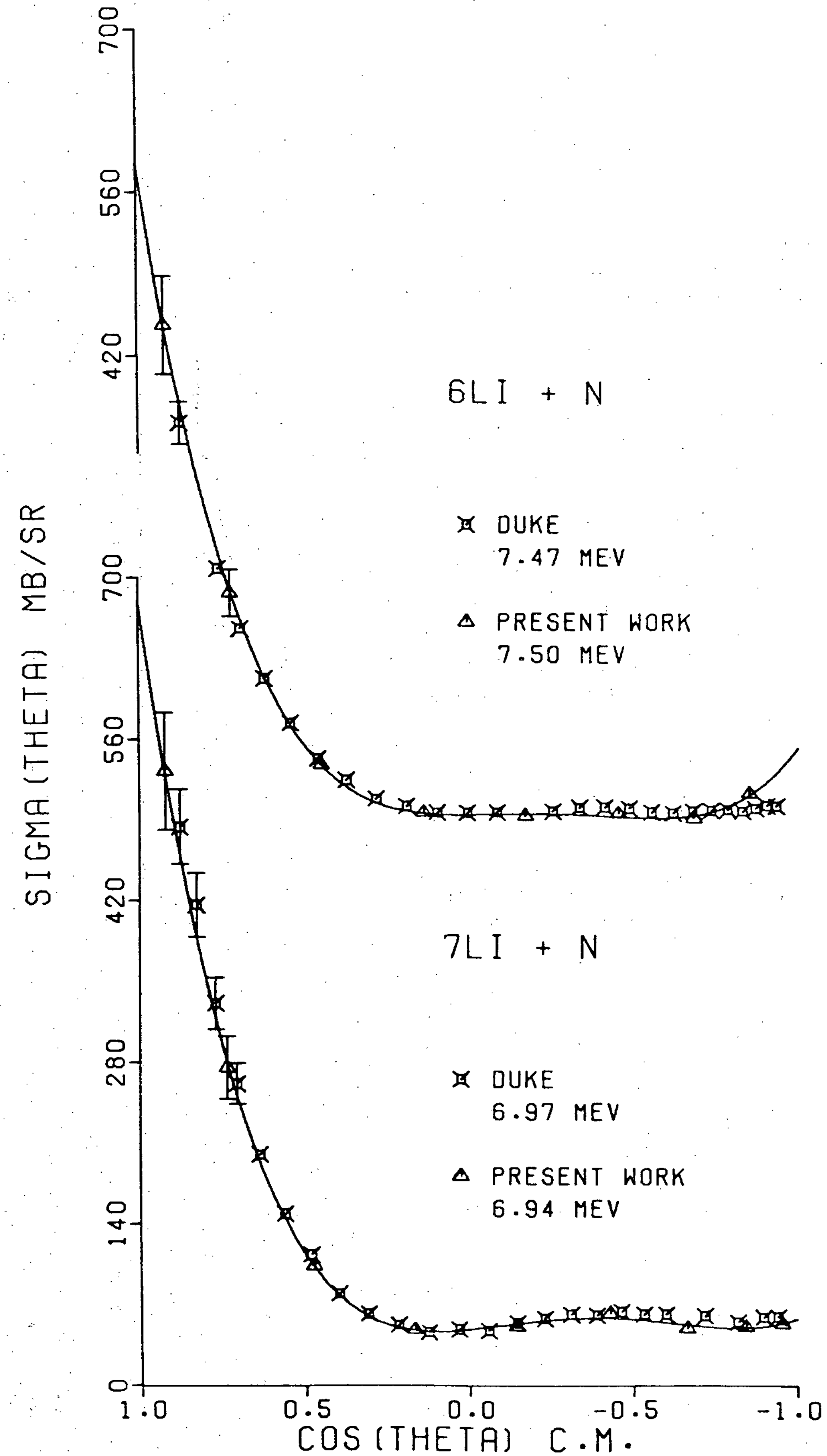
700
560
420
700
560
420
280
140
0
SIGMA(THETA) MB/SR
6LI + N
DUKE
7.47 MEV
PRESENT WORK
7.50 MEV
7LI + N
DUKE
6.97 MEV
PRESENT WORK
6.94 MEV
1.0
0.5
0.0
-0.5
-1.0
COS(THETA) C.M.
Figure 12.

6LI + N

CROSS SECTIONS AND ERRORS, C.M. (MB/SR)

ENERGY LAB (MEV)	ANGLE, C.M. (DEG) 23.2	43.3	62.9	81.7	99.6	116.7	132.9	148.3	163.2
4.08	319.5 20.9	201.6 13.5	108.7 7.6	63.9 5.0	53.1 4.3	48.9 4.0	57.8 5.1	72.6 6.6	95.9 8.4
4.26	354.2 23.2	213.1 14.2	107.8 7.5	57.1 4.4	47.7 3.8	44.1 3.8	51.2 4.8	69.1 6.3	89.5 8.0
4.57	371.2 24.5	212.3 14.3	109.5 7.7	51.8 4.1	39.1 3.3	38.9 3.5	45.3 4.4	56.7 5.4	75.1 6.9
4.83	373.4 24.9	213.3 14.4	95.7 6.8	48.1 3.8	40.6 3.4	38.9 3.5	38.9 3.7	51.3 4.9	73.8 6.7
5.05	402.1 26.8	220.5 14.8	96.1 6.8	44.8 3.4	37.4 3.1	37.4 3.3	37.5 3.4	53.9 4.8	68.5 5.8
5.29	410.5 27.0	227.1 15.1	93.6 6.5	45.5 3.5	35.2 2.9	34.8 3.0	42.5 3.6	50.5 4.5	63.2 5.4
5.54	410.7 26.7	232.3 15.4	94.1 6.6	41.7 3.2	34.3 2.9	34.6 2.9	38.4 3.2	48.2 4.0	60.6 5.0
5.74	447.6 29.0	234.9 15.8	95.4 6.8	41.5 3.2	32.2 2.7	36.4 3.0	36.4 3.1	45.8 3.8	56.9 4.7
6.05	436.5 28.7	220.4 15.2	87.3 6.3	37.3 3.0	30.6 2.6	30.4 2.6	32.7 2.9	43.0 3.5	48.9 4.0
6.37	418.6 27.7	222.0 15.3	81.3 5.8	32.5 2.7	28.7 2.5	26.9 2.4	27.8 2.6	33.0 2.8	36.8 3.2
6.66	434.4 28.7	219.5 14.9	73.8 5.6	34.8 2.9	27.2 2.4	27.5 2.4	24.8 2.4	35.2 3.1	35.9 3.1
6.94	432.9 28.7	210.6 14.4	71.8 5.4	28.5 2.5	21.4 1.8	28.6 2.6	21.1 2.0	26.3 2.6	35.3 3.2
7.32	416.6 28.2	208.6 14.0	66.6 5.2	23.5 2.0	20.8 1.8	18.6 1.8	15.4 1.7	25.4 2.4	40.7 3.8
7.50	446.5 30.0	213.9 14.5	65.0 5.2	23.4 2.2	19.8 1.8	21.2 2.0	17.1 1.8	38.0 3.2	

6LI + N

LEGENDRE COEFFICIENTS AND ERRORS, C.M.

(MB/SR)

ENERGY LAB (MEV)	B0	B1	B2	B3	B4
4.08	106.00	103.36	116.77	40.54	25.70
	2.95	6.51	8.10	8.45	8.05
4.26	106.49	118.02	133.46	52.35	30.14
	3.06	6.97	8.57	8.61	7.87
4.57	103.09	128.09	137.22	55.98	24.81
	3.10	7.15	8.72	8.60	7.48
4.83	100.19	129.36	141.66	69.33	38.03
	3.06	7.13	8.72	8.42	7.10
5.05	102.00	138.40	153.23	76.56	38.24
	3.16	7.47	8.99	8.50	6.82
5.29	102.19	140.71	153.69	76.22	32.18
	3.16	7.53	9.07	8.44	6.68
5.54	101.78	144.91	158.05	81.32	34.35
	3.16	7.50	8.94	8.26	6.44
5.74	104.59	154.87	167.33	89.86	36.27
	3.32	7.92	9.42	8.60	6.41
6.05	97.77	148.71	160.04	87.64	35.96
	3.20	7.71	9.13	8.26	6.02
6.37	92.53	149.30	155.89	91.38	35.23
	3.11	7.49	8.79	7.84	5.51
6.66	91.56	148.78	156.08	93.34	38.78
	3.11	7.55	8.95	8.00	5.42
6.94	87.89	150.39	160.07	97.10	39.85
	3.04	7.37	8.71	7.58	4.91
7.32	83.83	148.82	163.21	97.23	49.88
	2.96	7.15	8.37	6.99	4.78
7.50	82.80	150.55	151.96	96.89	28.84
	3.07	7.50	8.64	7.45	4.55

7LI + N
CROSS SECTIONS AND ERRORS, C.M. (MB/SR)

ENERGY LAB (MEV)	ANGLE, C.M. (DEG)								
	22.8	42.5	61.7	80.3	98.2	115.3	131.7	147.5	162.8
4.08	473.2 30.8	277.8 19.3	159.2 11.6	111.9 8.3	116.3 8.5	125.2 9.4	169.4 12.4	228.4 16.2	275.4 19.8
4.26	517.6 33.6	303.3 20.5	152.7 10.9	118.5 8.6	119.3 8.5	136.5 10.0	175.4 12.7	231.5 16.4	274.0 19.8
4.57	573.4 37.0	315.4 21.2	147.3 11.0	101.8 7.9	120.9 8.6	139.4 10.1	165.2 12.0	205.7 14.9	247.8 18.1
4.83	596.0 38.3	312.3 21.0	140.1 9.9	95.7 7.0	114.3 8.2	133.4 9.7	115.7 8.7	182.0 13.2	205.2 15.2
5.05	610.9 40.1	322.3 22.0	138.4 9.9	91.9 6.6	106.5 7.8	132.3 9.4	145.2 10.4	161.0 11.7	180.5 13.2
5.29	558.1 37.1	297.9 20.6	137.6 9.6	86.7 6.3	96.7 7.0	116.0 8.3	122.1 8.8	132.4 9.7	147.2 10.9
5.54	509.4 34.6	276.3 19.5	121.4 9.1	75.4 5.6	88.9 6.6	96.3 7.0	97.8 7.2	102.3 7.8	112.8 8.7
5.74	539.6 36.7	303.8 21.3	124.6 9.3	69.1 5.3	77.8 5.8	85.9 6.3	86.2 6.6	83.4 6.6	88.2 7.2
6.05	570.4 38.5	309.9 21.7	124.2 9.4	65.9 5.2	66.0 5.2	72.6 5.6	72.2 5.6	70.3 5.8	106.4 6.7
6.37	591.1 39.9	315.8 22.0	120.9 9.0	56.8 4.7	62.2 4.7	76.7 5.7	68.6 5.4	62.3 5.4	65.1 5.8
6.66	541.4 37.0	291.3 20.5	114.1 8.6	55.1 4.7	56.5 4.5	64.5 4.9	58.7 4.9	56.9 5.2	57.7 5.4
6.94	532.6 36.5	275.8 19.4	104.4 8.0	48.6 4.2	51.5 4.2	62.9 4.8	50.1 4.4	51.1 4.8	53.9 5.3
7.32	487.5 34.5	254.1 18.0	96.5 7.4	42.1 3.6	46.7 4.0	51.9 4.2	47.1 4.2	43.1 4.1	35.6 4.3
7.50	488.7 34.5	264.0 18.8	91.5 7.3	42.1 4.1	42.0 3.6	49.4 4.3	43.7 4.4	51.0 5.3	

7LI + N

LEGENDRE COEFFICIENTS AND ERRORS, C.M. (MB/SR)

ENERGY LAB (MEV)	B0	B1	B2	B3	B4
4.08	191.07	75.69	199.85	55.79	51.85
	4.74	10.15	12.71	13.72	14.95
4.26	200.30	87.35	215.26	78.28	60.44
	4.93	10.75	13.47	14.21	15.16
4.57	199.65	111.05	231.70	116.37	68.02
	5.06	11.20	13.95	14.65	15.13
4.83	187.97	138.48	229.83	131.58	90.41
	4.88	10.93	13.69	14.19	13.49
5.05	188.86	141.05	228.52	143.96	60.39
	5.00	11.39	13.90	14.27	13.66
5.29	171.31	140.54	200.94	127.02	50.37
	4.60	10.47	12.81	13.19	12.26
5.54	150.89	139.61	180.22	123.65	52.03
	4.25	9.69	11.80	12.14	10.93
5.74	149.15	165.18	193.06	133.78	47.96
	4.40	10.21	12.27	12.22	10.35
6.05	147.07	180.69	213.66	133.09	66.45
	4.46	10.46	12.61	12.23	9.83
6.37	144.30	191.68	213.30	152.07	51.84
	4.50	10.65	12.70	12.13	9.36
6.66	131.84	178.18	192.70	132.33	46.54
	4.19	9.92	11.89	11.38	8.78
6.94	124.61	174.54	191.07	135.14	51.91
	4.03	9.56	11.45	10.88	8.30
7.32	112.09	161.79	170.78	123.09	38.60
	3.75	8.94	10.58	10.02	7.62
7.50	110.31	163.04	170.34	121.33	32.50
	3.80	9.14	10.88	10.26	7.63